

Electronic Supplementary Information (ESI)

A data-driven approach to control stimulus responsivity of functional polymer materials:

Predicting thermoresponsive color-change properties of polydiacetylene

Risako Shibata,^a Nano Shioda,^a Hiroaki Imai,^a Yasuhiko Igarashi,^b Yuya Oaki*,^a

^a Department of Applied Chemistry, Faculty of Science and Technology, Keio University, 3-14-1 Hiyoshi, Kohoku-ku, Yokohama 223-8522, Japan.

^b Faculty of Engineering, Information and Systems, University of Tsukuba, 1-1-1 Tennodai, Tsukuba 305-8573, Japan

E-mail: oakiyuya@appc.keio.ac.jp

Contents

Experimental methods	P. S2
List of the guest molecules (Table S1)	P. S4
Datasets for ML (Tables S2 and S3)	P. S8
XRD patterns (Fig. S1)	P. S10
FT-IR spectra (Fig. S2)	P. S12
T – Δx relationship and its approximation (Fig. S3)	P. S13
Correlation analysis of x_{Gn} (Fig. S4)	P. S20
Five-fold cross validation (Fig. S5)	P. S21
List of the new guest molecules (Table S4)	P. S22
Structural analysis for the new layered PDAs (Fig. S6)	P. S23
T – Δx relationship for the new layered PDAs (Fig. S7)	P. S24

Experimental methods

Synthesis of the layered PDA with the intercalation of new guests: The guest molecules with the superscripted notes “*a–f*” in Table S1 were newly used in the present work. All these new guest amines were purchased from TCI with the purity higher than 95 %. These materials were used without further purification. The synthetic methods were referred to that in our previous works.^{45–52} The monomer solutions containing 8.83 mmol dm^{−3} PCDA (TCI 97.0 %) were prepared with ethanol, acetone, chloroform, or toluene. The already polymerized red-color precipitate was removed by the filtration. The guest amines were added and dissolved in the 6 cm³ of the monomer solutions with the following concentrations: 8.83 mmol dm^{−3} for the monoamine guests and 4.42 mmol dm^{−3} for the diamine guests. The molar ratio of the amino group to carboxy group was adjusted to 1.0 for all the guests. After mixing for 30 min, the solvent was evaporated at room temperature under ambient pressure. The resultant precipitate was polymerized with the UV irradiation using a handy lamp (6 W, 254 nm) for ca. 10 s.

Structural characterization: An increase in the interlayer distance was measured using XRD (Bruker, D8-Advance) with Cu-K α radiation. The changes in the carboxy and amino groups in the interlayer space were analyzed by KBr method using FT-IR (Jasco, FT/IR 4200).

Thermoresponsive color-change properties: The powder sample was filled in a stainless plate with a groove 5 × 7.5 mm in size. The plate was heated using a temperature-controlled stage, maintained at T °C to take a photograph using iPhone 13, and then heated again. The temperature range for the measurement was –50–250 °C depending on the guests. This cycle was repeated to observe the thermoresponsive color changes of the newly synthesized samples.

Preparation of datasets: The data about the thermoresponsive color-change properties were extracted from our previous works.^{45–51} The layered PDA with intercalating new guests was added in the present work. The registry numbers with S---, molecular structures, and their sources were listed in Table S1.

The color in the photographs was converted to the red-color intensity (x) based on the RGB values using an international standard using Eqs. (S1) and (S2).

$$\begin{bmatrix} X \\ Y \\ Z \end{bmatrix} = \begin{bmatrix} 0.4124 & 0.3576 & 0.1805 \\ 0.2126 & 0.7152 & 0.0722 \\ 0.0193 & 0.1192 & 0.9505 \end{bmatrix} \begin{bmatrix} R \\ G \\ B \end{bmatrix} \dots \text{Eq. (S1)}$$

$$(x, y) = \left(\frac{X}{X+Y+Z}, \frac{Y}{X+Y+Z} \right) \dots \text{Eq. (S2)}$$

An increment of x ($\Delta x = x - x_0$) was calculated to the initial state (x_0) at each T . Then, Δx was normalized by dividing the maximum Δx_{\max} ($\Delta x / \Delta x_{\max}$) in each sample because the Δx value was varied by the intensity of the color. This normalization is needed to compare the thermoresponsivity for each sample. The relationship between T and $\Delta x / \Delta x_{\max}$ was prepared for each layered PDA containing 75 different guests (Fig. S3). The T –($\Delta x / \Delta x_{\max}$) curve was approximated to a sigmoidal function Eq. (1) using the two constants a and b with a specific coefficient of determination (r^2). In this approximation, the coefficients a and b were adjusted to achieve the highest r^2 value for each guest. Then, the color-transition temperature (T_{trs}) was defined as T to reach $0.5\Delta x / \Delta x_{\max}$ in the fitting function Eq. (1) namely ($T_{\text{trs}} = a$). The explanatory variables (x_{Gn} : $n = 1$ –17) were calculated using the following applications (Table 1): HSP-ip (version 5.0.03), RDKit (2017.03.1), and Gaussian 16W by density functional theory (DFT) with B3LYP based on the 6–311G basis set. These data were summarized in Tables S2 and S3, supplied as CSV files.

Construction of the predictor: The datasets in Table S2 and S3 were used for training and test, respectively. The correlation coefficients in the training dataset were calculated in the training dataset (Table S2). The coefficients were color-coded to check the multicollinearity (Fig. S4). ES-LiR was performed on the dataset after removing x_{G5} , x_{G6} , x_{G9} , and x_{G10} . Linear regression models were exhaustively prepared for all the possible combinations of x_{Gn} ($2^n - 1$ patterns), such as $\{x_{G1} \text{ only}\}$, $\{x_{G1}, x_{G2}\}$, $\{x_{G1}, x_{G3}\}$, ..., $\{x_1, x_{Gn}\}$, $\{x_{G2} \text{ only}\}$, $\{x_{G2}, x_{G3}\}$, ..., $\{x_{Gn-1}, x_{Gn}\}$, $\{x_{G1}, x_{G2}, x_{G3}\}$, $\{x_{G1}, x_{G2}, x_{G4}\}$, ... $\{x_{G1}, x_{G2}, \dots, x_{Gn}\}$. The resultant models were sorted in the ascending order of the CVE values. The coefficients were visualized in the weight diagram. The descriptors were selected based on the weight diagram and our chemical insight. The model was prepared using the selected x_{Gn} and then validated using the test dataset (Table S3). The five-fold cross validation was carried out using the merged datasets of the original and test datasets (Tables S2 and S3). All these algorithms were implemented in Python. The implement method and code were available at GitHub of our group. Please see Data Availability in the main text.

List of the guest molecules

Table S1 summarizes the guest molecules intercalated in the layered PDA. The registry number, such as S---, was indexed in our group. The guest molecules with the superscripted notes “*a*–*f*” in Table S1 were newly used in the present work. The other guests were referred to our previous reports noted at the Table title. The XRD patterns and FT-IR spectra were summarized to show the characterization of the layered structures in Figs. S1 and S2, respectively. The notes *a*–*f* correspond to the panels in Figs. S1 and S2. The relationship between *T* and Δx for all the samples was summarized in Fig. S3.

Table S1-1. Guest molecules (25 linear alkyl amines) for training data.⁴⁵

S005	S006	S007	S008	S009	S010
Methylamine	Ethylamine	Propylamine	Butylamine	Amylamine	Hexylamine
S011	S012	S013	S014		
Heptylamine	<i>n</i> -Octylamine	Nonylamine	1-Aminodecane		
S015	S016	S017			
1-Aminoundecane	Dodecylamine	1-Aminotridecane			
S018	S019				
Tetradecylamine	1-Aminopentadecane				
S020	S021	S022			
Starylamine	1,4-Diaminobutane	1,6-Diaminohexane			
S023	S024	S025			
1,8-Diaminoctane	1,12-Diaminododecane	Dibutylamine			
S026	S027				
Dihexylamine	Di- <i>n</i> -octylamine				
S028	S029				
Didecylamine	Didodecylamine				

Table S1-2. Guest molecules (two branched alkyl amines) for training data.⁴⁵

S119^a 2-Heptylamine	S121^a 2-Methylbutylamine

Table S1-3. Guest molecules (three polymers) for training data.^{48,50}

S047^a Polyethylenimine, branched	S048 Polyethylenimine, linear
	S049 Poly(allylamine)

Table S1-4. Guest molecules (four amino-alcohols) for training data.

S054^a (S)-(+)-2-Amino-1-propanol	S056^a (R)-(-)-2-Amino-1-propanol	S058^a (S)-3-Amino-1,2-propanediol	S060^a (R)-3-Amino-1,2-propanediol

Table S1-5. Guest molecules (eight amines containing benzene ring) for training data.^{46,51}

S069 Benzylamine	S070^b 2-Phenylethylamine	S071^b 3-Phenylpropylamine	S073 <i>p</i> -Xylylenediamine	S074^b <i>m</i> -Xylylenediamine
S075^b Benzhydrylamine	S077^b Tyramine	S078^b Tryptamine		

Table S1-6. Guest molecules (nine amines containing cycloalkane rings) for training data.

S145^c Cyclohexylamine (cC6amine)	S146^c Cyclooctylamine (cC8amine)	S147^c Hexamethyleneimine (cC6imine)	S150^c <i>cis</i> -1,3-Cyclohexanediamine (<i>cis</i> - <i>m</i> -cC6di)
S152^c 4,4'-Methylenebis(cyclohexylamine) (mixture of isomers)	S153^c Cyclopropylamine (cC3amine)	S154^c Aminocyclobutane (cC4amine)	S155^c Cyclohexanemethylamine (cC6methylamine)
S157^c cis-1,4-Cyclohexanediamine (cis-p-cC6di)	S158^c trans-1,4-Cyclohexanediamine (trans-p-cC6di)	S159^c cis-1,4-Bis(aminomethyl)cyclohexane	S160^c trans-1,4-Bis(aminomethyl)cyclohexane

Table S1-7. Guest molecules (five amines containing benzene ring) for training data.

S105^d 4-Methoxybenzylamine (<i>p</i> -OMeBA)	S106^d 2-Methoxybenzylamine (<i>o</i> -OMeBA)	S107^d 3-Methoxybenzylamine (<i>m</i> -OMeBA)	S108^d 1-Naphthylmethylamine (NpMeA)	S111^d 4-Fluorobenzylamine (FBA)

Table S1-8. Guest molecules (five amines containing heteroaromatic rings) for training data.⁴⁹

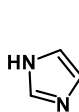
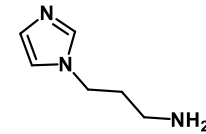
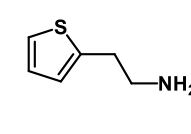
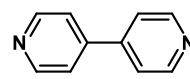
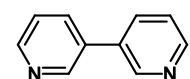
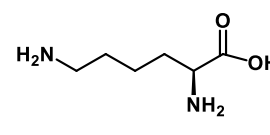
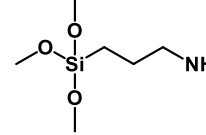
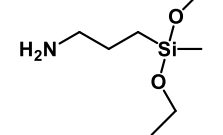
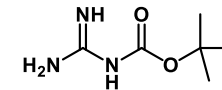
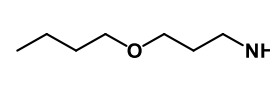
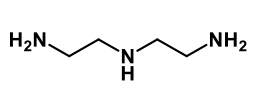
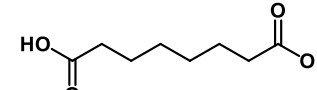
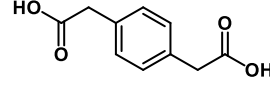
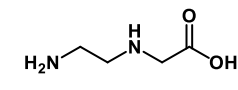
				
S033^e Imidazole	S035^e 1-(3-Aminopropyl)imidazole	S110^e 2-(2-Aminoethyl)thiophene (AEtTp)	S128 4,4'-Bipyridyl	S131 3,3'-Bipyridyl

Table S1-9. Guest molecules (ten other amines) for training data.⁴⁷

			
S041 L-(+)-Lysine	S066^f 3-Aminopropyltrimethoxysilane	S067^f 3-Aminopropyldiethoxymethylsilane	S083 1-(4-Cyanophenyl)guanidine
			
S085 1-(tert-Butoxycarbonyl)guanidine	S088^f 3-Butoxypropylamine	S112^f Diethylenetriamine	S140^f Suberic acid
			
S142^f 1,4-Phenylenediacetylacid	S161^f N-(2-Aminoethyl)glycine		

Datasets for ML

Table S2. Training dataset containing 65 y.

	x_{G1}	x_{G2}	x_{G3}	x_{G4}	x_{G5}	x_{G6}	x_{G7}	x_{G8}	x_{G9}	x_{G10}	x_{G11}	x_{G12}	x_{G13}	x_{G14}	x_{G15}	x_{G16}	x_{G17}	T_{ts}
S005	17.11	7.71	13.02	0.656	47.3	65.46	-22	-71	1.035	31.058	-0.4251	26.02	2.958	-0.695	19.6	1.3014	1	57.58
S006	15.8	6.34	10.04	0.7	64.4	87.31	16	-82	1.123	45.085	-0.035	26.02	3.796	-0.686	31.45	1.2858	1	48.89
S007	15.71	5.15	8.33	0.723	81.8	108.95	48	-79	1.196	59.112	0.3551	26.02	5.292	-0.697	42.56	1.2265	1	49.61
S008	15.82	4.6	8.38	0.738	99.1	131.19	77	-65	1.267	73.139	0.7452	26.02	6.301	-0.696	53.85	1.2516	1	35.74
S010	15.99	3.94	7.48	0.769	131.6	174.69	133	-50	1.397	101.193	1.5254	26.02	8.258	-0.663	76.8	1.237	1	59.45
S011	16.01	3.89	6.12	0.778	148.1	196.89	156	-27	1.455	115.22	1.9155	26.02	7.139	-0.696	88.21	1.2091	1	50.62
S012	16.04	3.18	5.39	0.783	165	219.14	178	-14	1.506	129.247	2.3056	26.02	8.883	-0.663	99.37	1.2549	1	63.32
S013	16.08	3.01	5.12	0.792	180.9	240.27	199	19	1.553	143.274	2.6957	26.02	10.451	-0.697	110.83	1.2425	1	51.16
S014	16.09	2.9	5.3	0.796	197.5	262.64	220	12	1.601	157.301	3.0858	26.02	11.322	-0.720	123	1.2399	1	73.86
S015	16.07	2.94	4.4	0.8	214	284.83	237	20	1.646	171.328	3.4759	26.02	12.071	-0.668	134.05	1.287	1	66.23
S016	16.08	2.42	3.95	0.802	231	307.08	252	42	1.687	185.355	3.866	26.02	12.489	-0.696	146.31	1.2382	1	99.59
S017	16.09	2.32	3.85	0.808	246.9	327.83	270	35	1.723	199.382	4.2561	26.02	13.939	-0.696	157.98	1.205	1	63.44
S018	16.07	2.26	4.12	0.81	263.5	350.58	288	42	1.764	213.409	4.6462	26.02	14.042	-0.696	169.67	1.2375	1	80.55
S019	16.05	2.34	3.42	0.812	280	372.78	303	57	1.801	227.436	5.0363	26.02	11.125	-0.696	181.36	1.2044	1	71.89
S020	16.03	1.82	3.36	0.818	329.5	438.53	345	71	1.901	269.517	6.2066	26.02	14.783	-0.696	216.47	1.2366	1	90.61
S021	17.01	6	10.27	0.864	102	148.88	160	14	1.41	88.154	-0.316	52.04	7.254	-0.696	60.86	0.0001	2	94.75
S022	16.76	5.26	9.62	0.864	134.5	192.38	203	27	1.516	116.208	0.4642	52.04	7.264	-0.696	83.79	1.8913	2	99.47
S023	16.57	4.39	6.49	0.859	168	236.82	236	-5	1.609	144.262	1.2444	52.04	10.054	-0.696	106.92	1.8934	2	99.83
S024	16.34	3.41	4.54	0.857	233.9	324.77	298	81	1.769	200.37	2.8048	52.04	12.991	-0.696	153.51	1.8928	2	99.59
S025	15.79	2.68	4.4	0.754	171.3	218.83	150	-42	1.467	129.247	2.1762	12.03	8.860	-0.541	101.21	0.889	1	68.25
S027	16	1.57	2.65	0.796	303.3	394.72	287	-3	1.809	241.463	5.297	12.03	14.945	-0.526	194.55	0.8706	1	49.84
S028	16.02	1.47	2.45	0.808	368.3	481.72	349	18	1.939	297.571	6.8574	12.03	15.730	-0.542	241.4	0.8683	1	60.36
S029	15.99	1.01	1.9	0.813	435.2	570.61	386	50	2.055	353.679	8.4178	12.03	22.514	-0.542	286.84	0.8807	1	58.56
S033	19.72	12.46	12.01	1.02	66.7	94.2	163	33	1.184	68.079	0.4097	28.68	4.257	-0.610	39	4.0312	1	47.51
S035	18.25	8.5	8.25	0.997	125.6	167.81	246	172	1.384	125.175	0.2319	43.84	7.046	-0.698	80.98	5.1453	2	68.75
S041	16.77	7.19	14.28	1.079	135.5	200.61	314	349	1.573	146.19	-0.4727	89.34	8.986	-0.690	86.55	0.4144	2	103.01
S048	16.51	4.17	6.44	0.905	286.6	396.23	317	-41	1.885	259.442	-0.6357	60.15	17.951	-0.551	245.04	0.9341	1	43.36
S049	16.61	3.72	5.92	0.952	346.1	474.76	524	227	1.992	329.577	1.2413	130.1	14.410	-0.736	322.88	1.1402	1	47.44
S056	17.27	8.48	17.62	0.95	79.1	115.2	163	-20	1.293	75.111	-0.6741	46.25	4.444	-0.702	46.29	1.0473	1	63.82
S058	18.34	10.9	22.51	1.154	78.9	128.98	248	17	1.45	91.11	-1.7017	66.48	5.624	-0.697	48.56	2.466	1	83.67
S060	18.34	10.9	22.51	1.154	78.9	128.98	248	17	1.45	91.11	-1.7017	66.48	5.417	-0.676	48.55	1.9734	1	79.26
S066	14.23	4.23	5.43	0.983	182.3	248.06	178	58	1.596	179.292	0.2133	53.71	8.461	-0.834	104.44	0.6564	1	82.01
S069	18.78	4.57	7.09	0.976	109.8	146.96	185	-2	1.325	107.156	1.1453	26.02	7.027	-0.685	77.57	1.4882	1	75.18
S070	18.38	4.26	7.06	0.958	126.4	168.93	207	-48	1.387	121.183	1.1878	26.02	7.188	-0.696	89.52	1.321	1	72.42
S071	18.06	3.93	5.75	0.946	142.9	191.13	225	-24	1.446	135.21	1.5779	26.02	8.091	-0.697	101.34	1.4195	1	48.11
S073	19.32	6.06	9.04	1.047	130.1	186.71	275	-30	1.504	136.198	0.604	52.04	8.266	-0.686	98.8	1.259	2	97.22
S074	19.14	5.35	8.05	1.045	130.4	186.78	278	-42	1.502	136.198	0.604	52.04	7.884	-0.686	97.97	0.1359	2	81.12
S077	19.15	6.66	12.88	1.068	128.4	180.88	284	37	1.469	137.182	0.8934	46.25	8.712	-0.696	94.75	1.2187	1	71.89
S078	19.81	7.17	8.75	1.112	144.1	202.15	321	143	1.521	160.22	1.6691	41.81	7.773	-0.735	117.7	2.878	1	53.26
S083	21.26	15.1	15.51	1.249	128.2	191.38	310	-90	1.557	160.18	-1.17022	85.64	9.513	-0.802	118.59	5.2605	1	40.35
S085	17.71	11.6	14.28	1.107	143.8	204.3	217	143	1.539	159.189	-1.6293	88.15	8.089	-0.773	95.09	3.5414	1	30.57
S088	16.09	5.06	6.96	0.842	155.8	209.36	172	-80	1.495	131.219	1.1519	35.25	9.380	-0.694	93.19	2.1838	1	50.98
S105	18.98	6.45	8.01	1.049	130.7	180.28	241	-15	1.448	137.182	1.1539	35.25	8.999	-0.685	96.15	1.3346	1	77.77
S106	18.87	6.03	7.51	1.05	130.7	179.67	225	-27	1.443	137.182	1.1539	35.25	7.059	-0.703	94.22	2.1774	1	71.92
S107	18.8	5.74	7.02	1.047	131	180.35	242	-31	1.446	137.182	1.1539	35.25	7.127	-0.686	95.11	2.584	1	87.81
S110	18.89	5.26	9.88	1.099	115.8	158.5	198	-12	1.38	127.212	1.2493	26.02	7.697	-0.699	84	2.1548	1	80.55
S111	18.73	6.18	7.27	1.094	114.4	155.41	183	2	1.364	125.146	1.2844	26.02	7.342	-0.683	77.57	3.609	1	92.61
S112	17.48	6.9	15.02	0.935	110.3	165.32	212	-9	1.486	103.169	-1.5066	64.07	7.894	-0.699	68.94	1.4154	2	72.99
S119	15.95	3.24	6.06	0.777	148.3	191.03	147	-48	1.41	115.22	1.9139	26.02	8.416	-0.660	88.44	1.1653	1	60.68
S131	20.2	7.5	5.71	1.138	137.3	183.28	285	67	1.424	156.188	2.1436	25.78	9.239	-0.250	114.66	1.5118	2	58.84
S140	16.81	7.4	15.02	1.106	157.5	228.26	344	105	1.619	174.196	1.4962	74.6	10.187	-0.542	99.28	2.3149	2	78.62
S142	18.97	7.78	15.99	1.268	153.1	225.9	386	182	1.609	194.186	0.9408	74.6	10.158	-0.539	114.55	2.7234	2	74.71
S145	17.19	3.61	6.07	0.864	114.8	157.35	141	-92	1.378	99.177	1.2778	26.02	5.775	-0.666	72.42	1.1895	1	55.02
S146	17.21	3.34	5.34	0.863	147.5	195.55	188	-40	1.449	127.231	2.058	26.02	6.288	-0.705	93.92	1.1495	1	44.95
S147	17.2	4.5	5.68	0.855	116	149.9	135	-23	1.304	99.177	1.15	12.03	5.227	-0.499	72.23	0.9897	1	44.51
S150	17																	

Table S3. Test dataset containing 10 y .

	x_{G1}	x_{G2}	x_{G3}	x_{G4}	x_{G5}	x_{G6}	x_{G7}	x_{G8}	x_{G9}	x_{G10}	x_{G11}	x_{G12}	x_{G13}	x_{G14}	x_{G15}	x_{G16}	x_{G17}	T_{rs}
S009	15.92	4.22	7.61	0.758	115	152.72	107	-53	1.336	87.166	1.1353	26.02	7.209	-0.665	65.05	1.2329	1	50.31
S026	15.99	2.27	3.59	0.784	236.4	305.83	227	-28	1.654	185.355	3.7366	12.03	13.456	-0.526	147.79	0.8758	1	51.39
S047	16.01	4.17	7.98	0.906	301.9	406.68	332	-4	1.869	273.469	-0.212	56.56	12.925	-0.703	336.58	3.0527	1	38.18
S054	17.27	8.48	17.62	0.95	79.1	115.2	163	-20	1.293	75.111	-0.6741	46.25	4.696	-0.661	46.25	2.8448	1	60.71
S067	14.33	3.75	4.01	0.902	212.1	275.59	208	33	1.603	191.347	1.4802	44.48	8.751	-0.997	126.62	3.2724	1	56.90
S075	18.99	3.02	4.87	1.054	173.8	223.72	309	66	1.486	183.254	2.7347	26.02	9.317	-0.701	137.26	1.1596	1	62.57
S108	19.97	4.71	6.61	1.087	144.7	167.64	284	111	1.258	157.216	2.2985	26.02	7.696	-0.698	122.84	1.6124	1	133.59
S121	15.67	3.68	6.16	0.753	115.8	148.29	96	-74	1.291	87.166	0.9912	26.02	6.159	-0.696	65.1	1.4741	1	84.94
S128	20.2	7.5	5.71	1.138	137.3	183.28	285	65	1.424	156.188	2.1436	25.78	7.875	-0.227	113.26	0	2	51.31
S155	17.11	3.44	5.68	0.872	129.8	175.86	165	-44	1.419	113.204	1.5254	26.02	6.805	-0.694	83.38	1.2931	1	33.81

XRD patterns

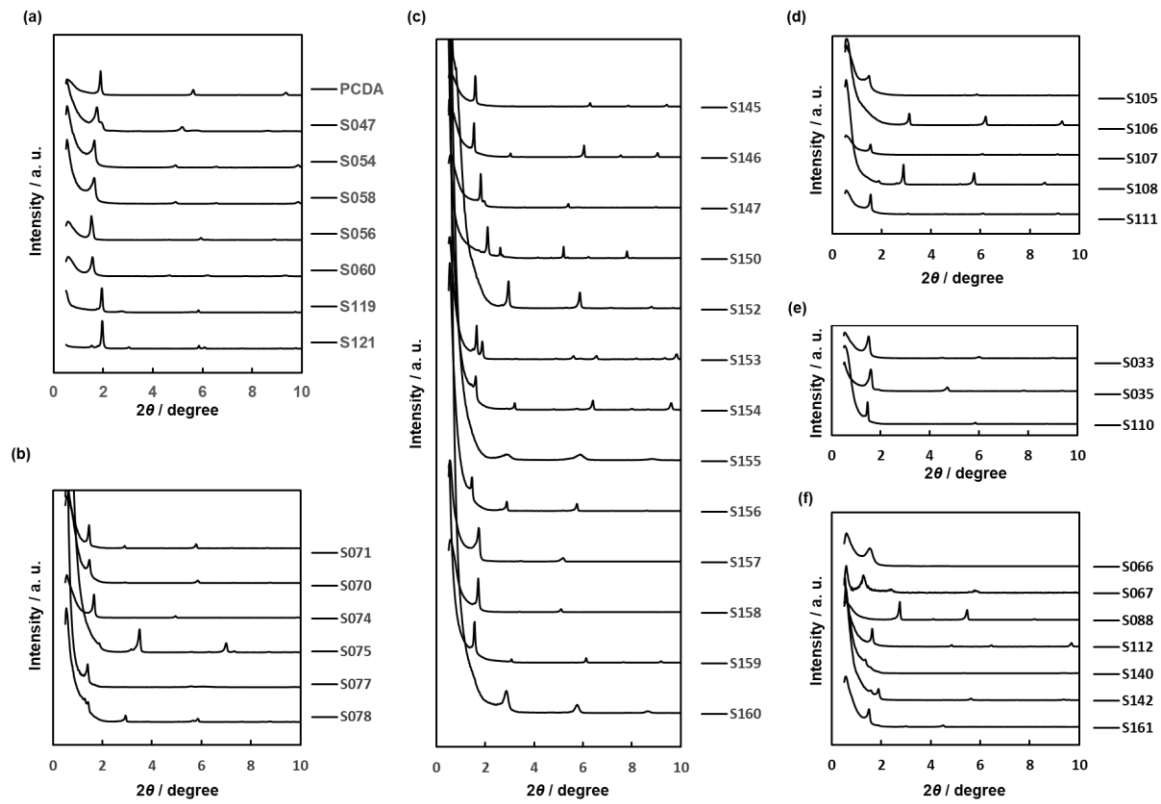


Fig. S1. XRD patterns of the newly synthesized layered PDA with the intercalation of the guests. (a) Polymeric and branched alkyl amines and amino-alcohols. (b) Amines containing benzene rings. (c) Amines containing cycloalkane rings. (d) Benzylamine derivatives. (e) Amines containing heteroaromatic rings. (f) Others.

The original PCDA without the guest showed the interlayer distance (d_0) = 4.66 nm. The peak shift indicating the intercalation of the guests was observed for all these guests. The observed d_0 was as follows: (a) 5.05 nm for **S047**, 5.38 nm for **S054**, 5.79 nm for **S058**, 5.39 nm for **S056**, 5.63 nm for **S060**, 3.21 nm for **S119**, 5.74 nm for **S121**. (b) 5.99 nm for **S071**, 6.06 nm for **S070**, 5.32 nm for **S074**, 5.12 nm for **S075**, 6.32 nm for **S077**, 7.23 nm for **S078**. (c) 5.55 nm for **S145**, 5.75 nm for **S146**, 4.87 nm for **S147**, 4.18 nm for **S150**, 5.98 nm for **S152**, 5.37 nm for **S153**, 5.50 nm for **S154**, 6.18 nm for **S155**, 6.08 nm for **S156**, 5.01 nm for **S157**, 5.16 nm for **S158**, 5.26 nm for **S159**, 5.40 nm for **S160**. (d) 6.02 nm for **S105**, 5.94 nm for **S106**, 5.80 nm for **S107**, 6.16 nm for **S108**, 5.75 nm for **S111**, (e) 5.88 nm for **S033**, 5.50 nm for **S035**, 6.03 nm for **S110**. (f) 6.07 nm for **S066**, 7.23 nm for **S067**, 3.21 nm for **S088**, 5.41 nm for **S112**, 6.51 nm for **S140**, 5.62 nm for **S142**, 5.88 nm for **S161**.

In some cases, such as **S088**, d_0 decreased after the intercalation. The longer alkyl chains of the guest generate the interdigitated states in the interlayer space (Fig. 1c). The original PCDA

has the similar interdigitated alkyl chains in the layered structure. The new periodicity originating from the interdigitated alkyl chains is generated with the intercalation of the guests. Such states were observed in our previous report.⁴⁴ The detailed analyses with changes in the alkyl chain length support the interpretation of a decrease in d_0 .⁴⁴

FT-IR spectra

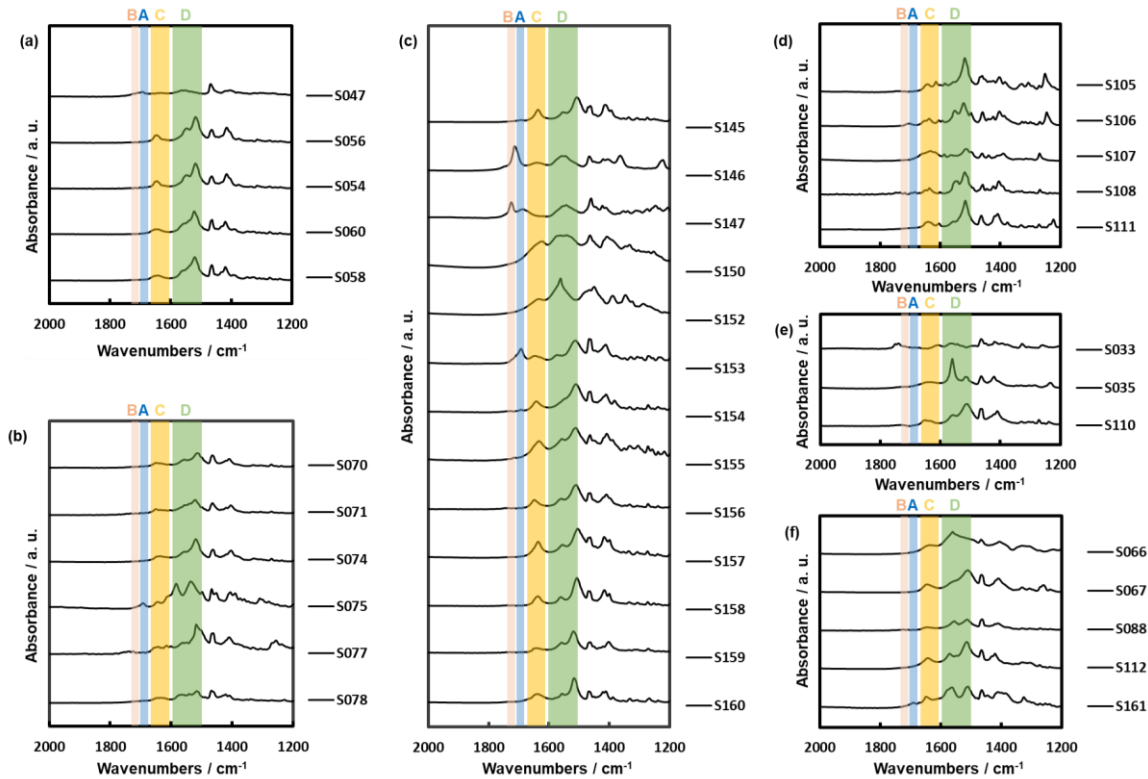


Fig. S2. FT-IR spectra of the newly synthesized layered PDA with the intercalation of the guests. (a) Polymeric and branched alkyl amines and amino-alcohols. (b) Amines containing benzene rings. (c) Amines containing cycloalkane rings. (d) Benzylamine derivatives. (e) Amines containing heteroaromatic rings. (f) Others.

The layered PDA without the interlayer guests only shows the absorption around 1690 cm^{-1} corresponding to the stretching vibration of $\text{C}=\text{O}$ group in the dimerized carboxy group (band A, blue). In most cases, the band A was not observed after the intercalation of the guests and the guest-intercalated PDAs showed the absorption in the range of $1600\text{--}1650\text{ cm}^{-1}$ corresponding to the stretching vibration of $\text{C}=\text{O}$ group in the dimerized carboxylate group (band C, yellow). The absorbance of the band A was drastically weakened in some cases, such as **S047** and **S075** (Fig. S2a,b). The absorption around 1700 cm^{-1} corresponding to the stretching vibration of $\text{C}=\text{O}$ group in the monomeric carboxy group was observed for other cases (band B, orange), such as **S146** and **S147** (Fig. S2c). The absorption in the range of $1550\text{--}1600\text{ cm}^{-1}$ correspond to the stretching vibration of NH group in the amine salt (band D, green). These changes in the carboxy and amine groups indicate the intercalation of the guest molecules in the interlayer space.^{45–52}

T - Δx relationship and its approximation

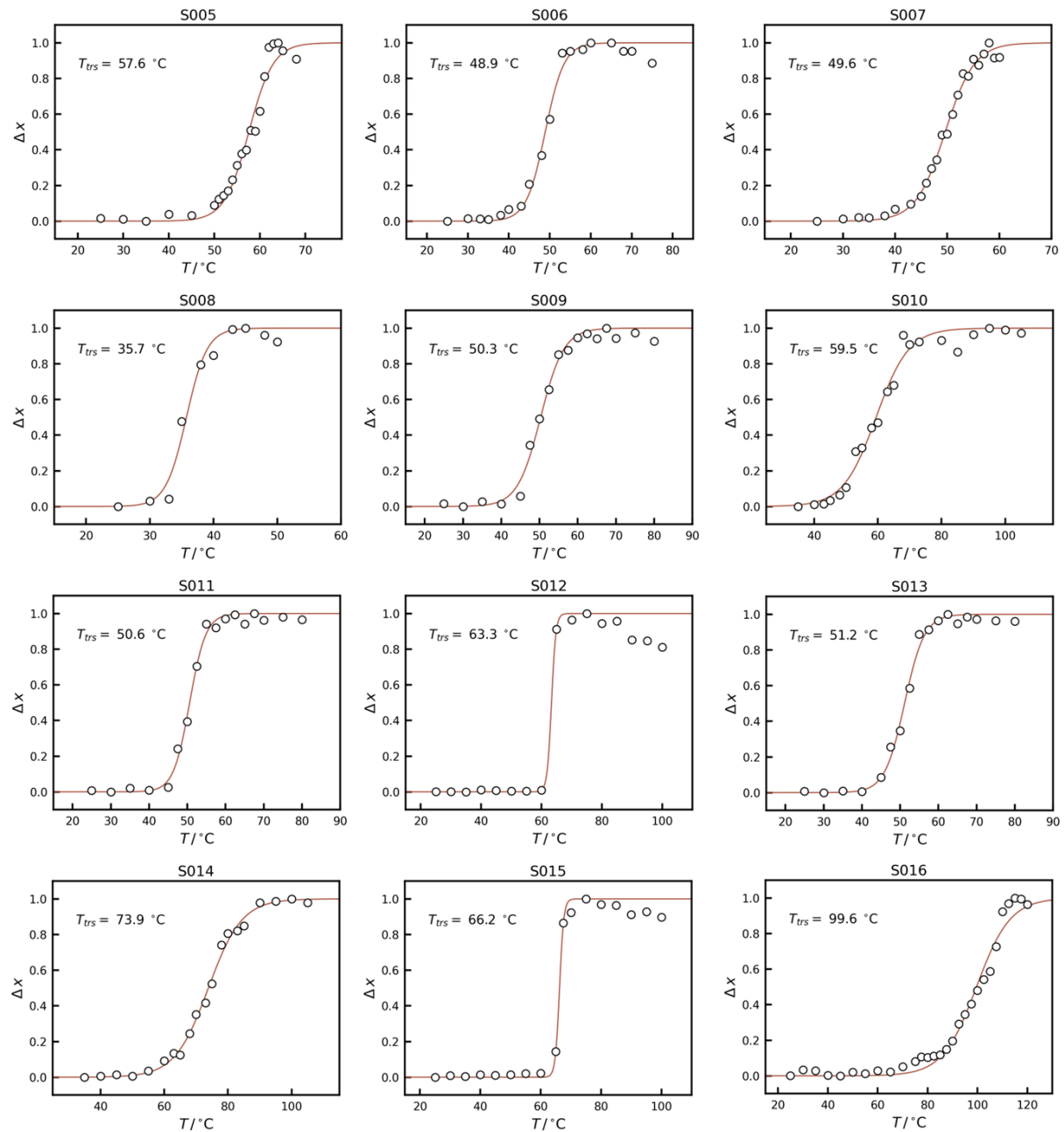


Fig. S3-1. T - Δx relationship (plot), its approximation using sigmoidal function (red line), and calculated T_{trs} for all the data (75 y) used for the model construction.

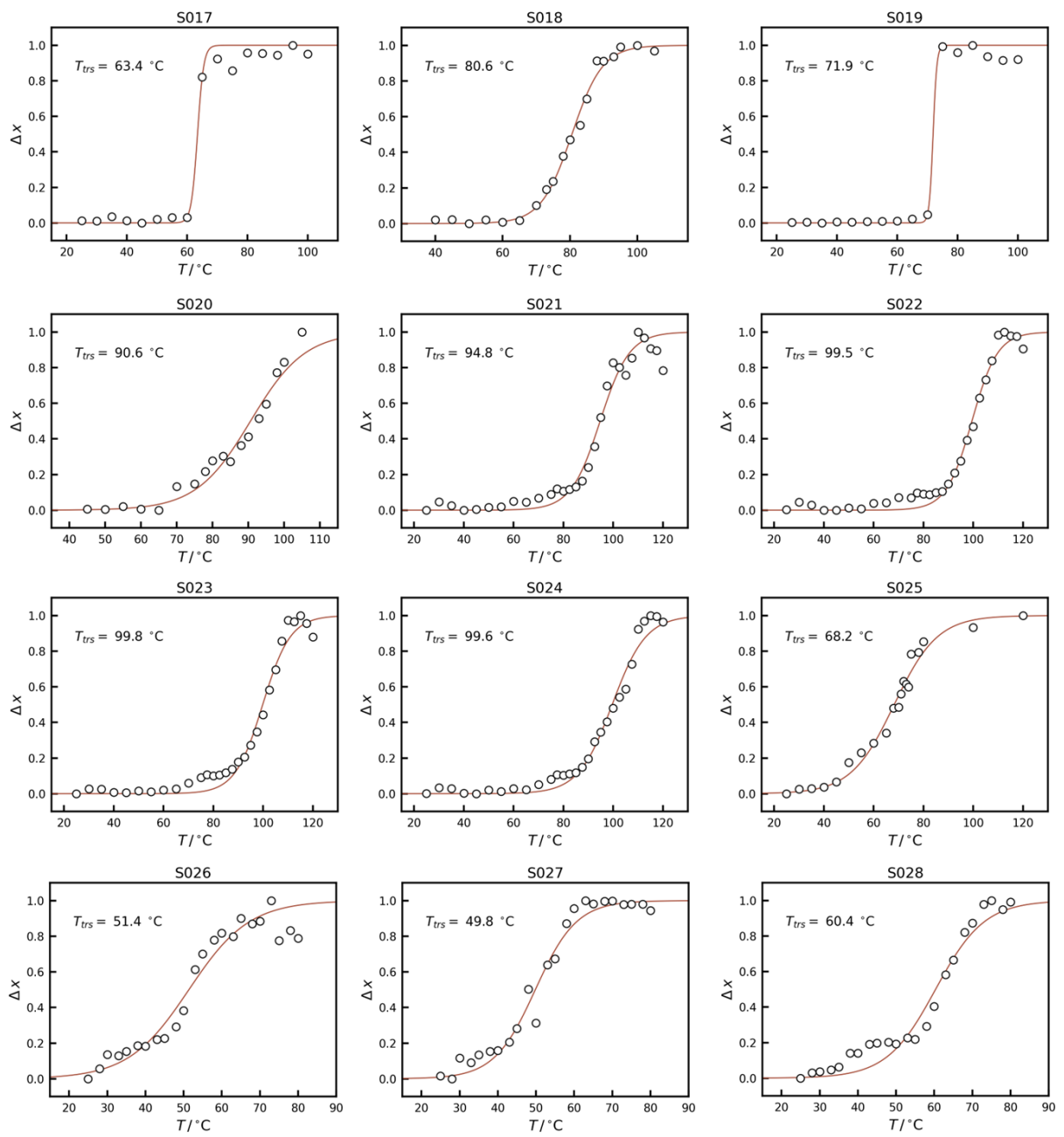


Fig. S3-2. (continued).

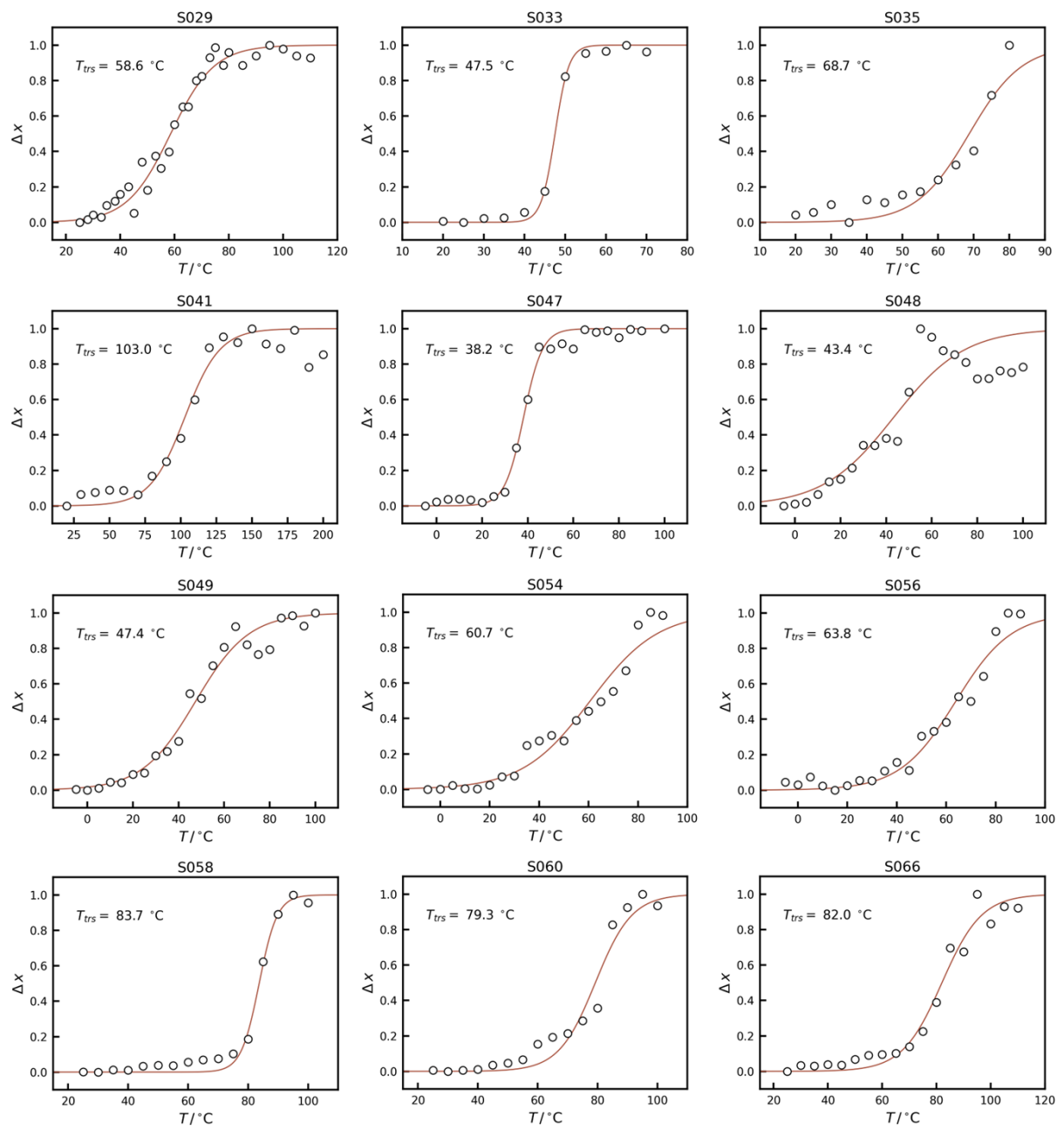


Fig. S3-3. (continued).

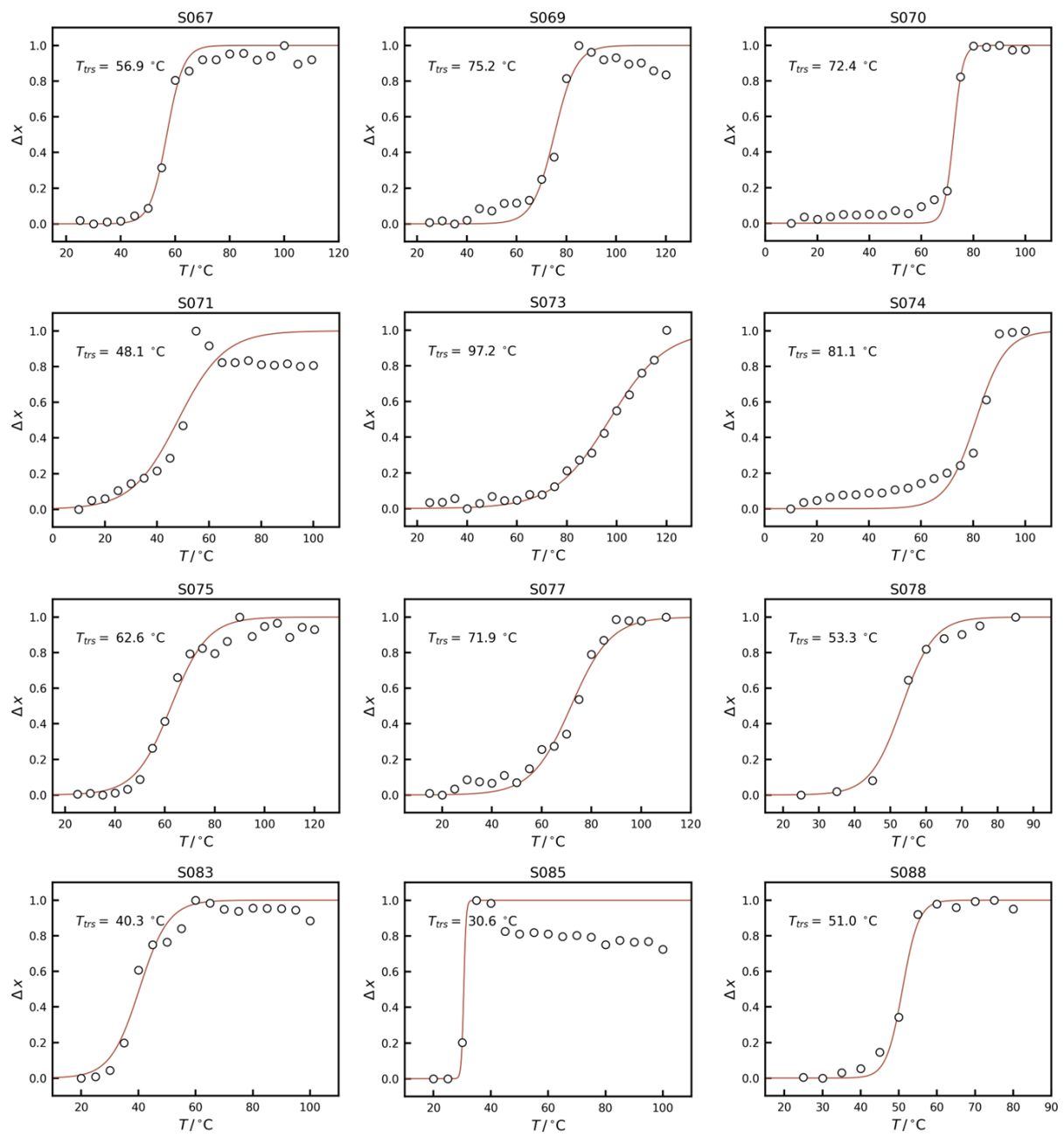


Fig. S3-4. (continued).

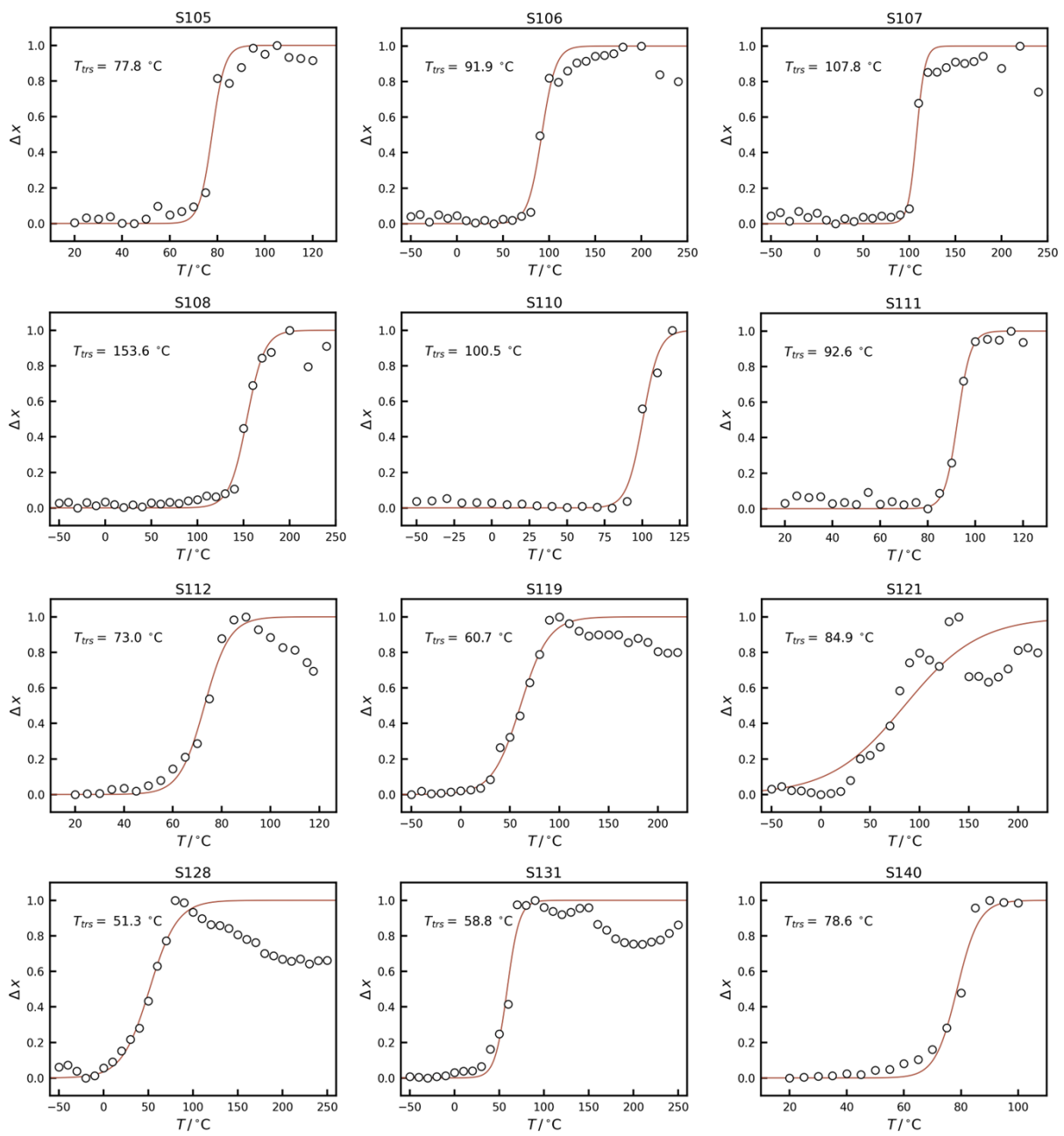


Fig. S3-5. (continued).

Note: The data of the samples S106, S107, S108, and S110 were corrected using the T_{trs} values of the reference PDA sample without intercalation of the guests. As such deviation is caused by the measurement conditions, the correction based on the reference samples is needed.

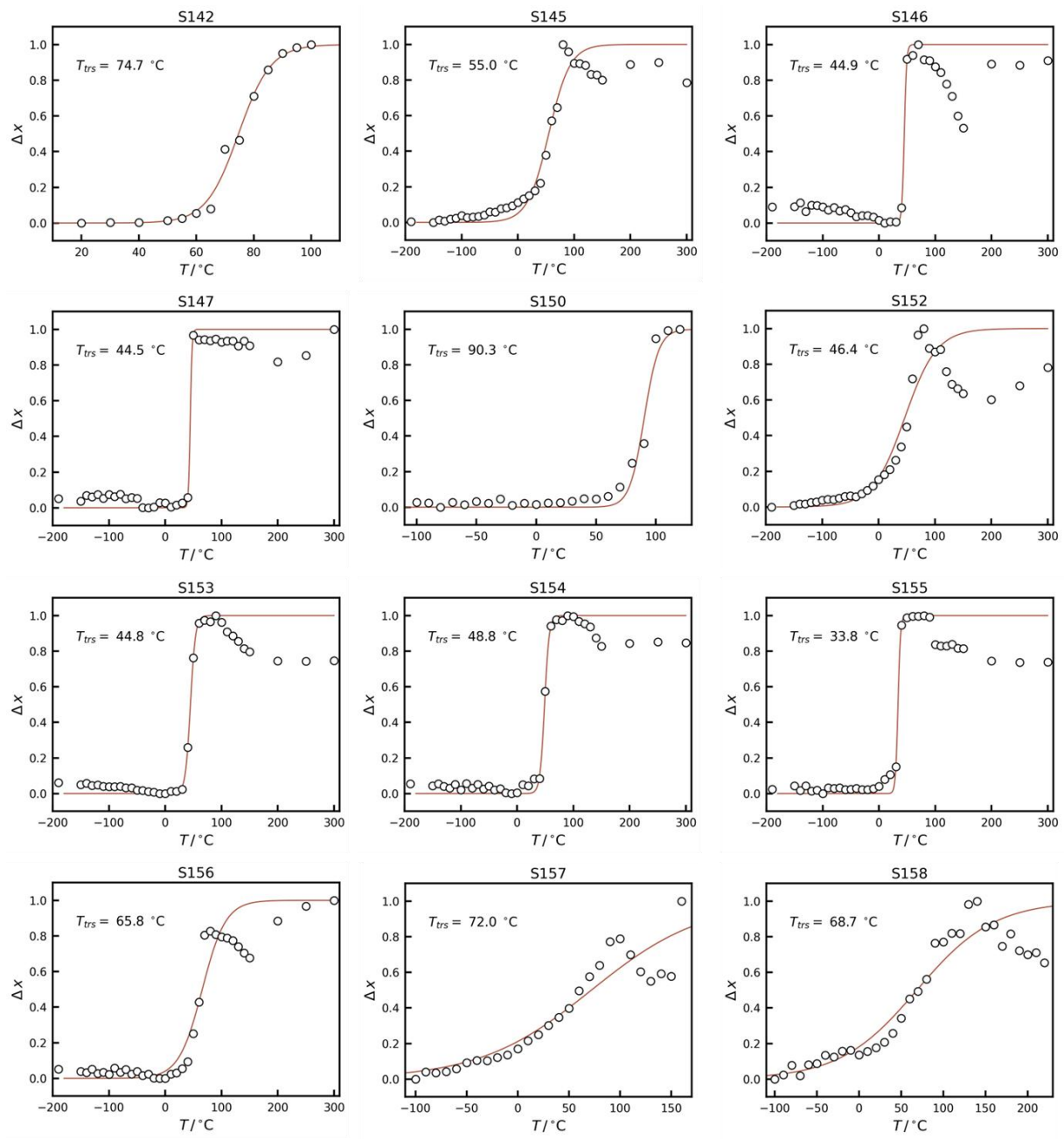


Fig. S3-6. (continued).

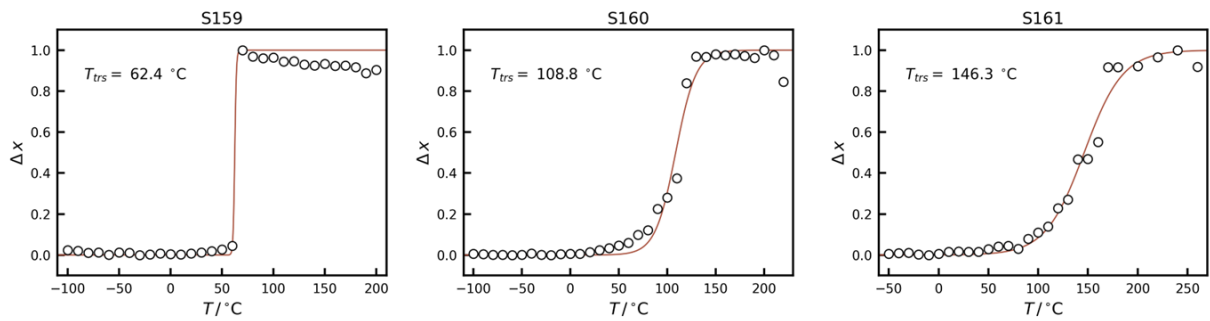


Fig. S3-7. (continued).

These observed T - Δx plots (circles) were approximated using Eq. (1) with adjusting a and b to minimize the r^2 value.

Table S4. List of the R^2 values for the approximation of all the T - Δx plots.

Fig. S3-1	S005	S006	S007	S008	S009	S010	S011	S012	S013	S014	S015	S016
	0.9719	0.9894	0.9931	0.9785	0.9900	0.9823	0.9944	0.9737	0.9937	0.9951	0.9907	0.9813
Fig. S3-2	S017	S018	S019	S020	S021	S022	S023	S024	S025	S026	S027	S028
	0.9883	0.9939	0.9939	0.9650	0.9698	0.9855	0.9796	0.9813	0.9817	0.9408	0.9741	0.9596
Fig. S3-3	S029	S033	S035	S041	S047	S048	S049	S054	S056	S058	S060	S066
	0.9748	0.9968	0.9091	0.9574	0.9917	0.8361	0.9728	0.9544	0.9637	0.9893	0.9603	0.9723
Fig. S3-4	S067	S069	S070	S071	S073	S074	S075	S077	S078	S083	S085	S088
	0.9824	0.9587	0.9865	0.8589	0.9851	0.9324	0.9760	0.9816	0.9894	0.9650	0.6291	0.9916
Fig. S3-5	S105	S106	S107	S108	S110	S111	S112	S119	S121	S128	S131	S140
	0.9748	0.9701	0.9598	0.9752	0.9778	0.9880	0.9422	0.9447	0.8217	0.6690	0.8972	0.9814
Fig. S3-6	S142	S145	S146	S147	S150	S152	S153	S154	S155	S156	S157	S158
	0.9911	0.9473	0.8686	0.9770	0.9735	0.8113	0.9422	0.9752	0.9328	0.9130	0.8790	0.8793
Fig. S3-7	S159	S160	S161									
	0.9896	0.9852	0.9842									

The average R^2 values were 0.952 ± 0.066 for all the data in Fig. S3. Based on the R^2 values and fitting results, the thermoresponsive color-changing properties are approximated by sigmoidal function to estimate T_{trs} .

Correlation analysis of x_{Gn}

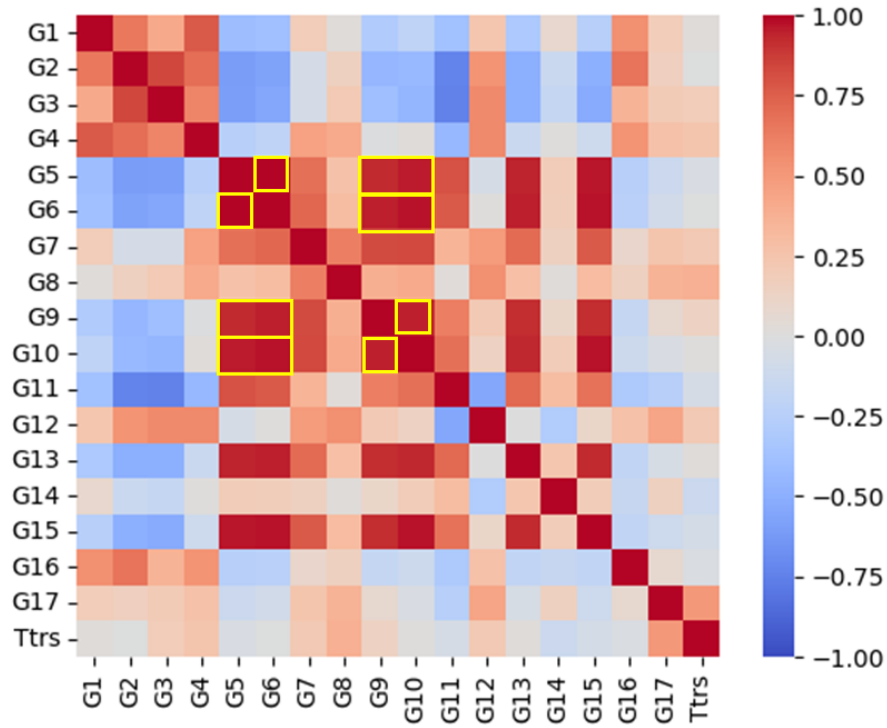


Fig. S4. Correlation analysis of 17 x_{Gn} .

The heatmap indicates that the correlation coefficients of x_{G5} , x_{G6} , x_{G9} , and x_{G10} were larger than 0.9 (yellow frames in Fig. S4).

Five-fold cross validation

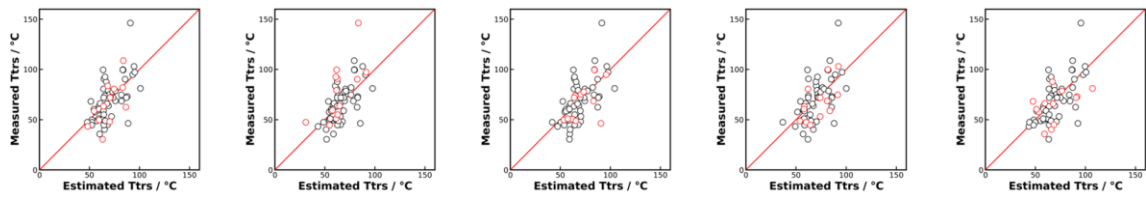
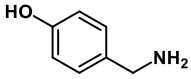
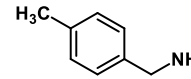
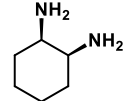
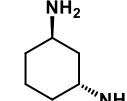
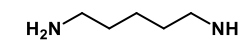
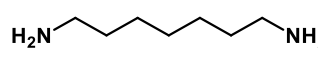
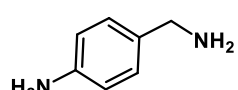
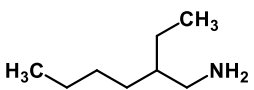
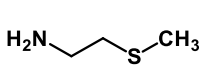


Fig. S5. Relationship between the estimated and measure T_{trs} for five-fold cross validation using the merged dataset of the original training and test ones (75 y).

This five-fold CV was carried out for the model consisting of the five x_{Gn} (x_{G4} , x_{G12} , x_{G14} , x_{G16} , and x_{G17}). The average RMSE was 15.6 ± 1.2 °C for training and 17.3 ± 4.1 °C for test.

List of the new guest molecules

Table S5. New guest molecules for the experimental validation of the model.

				
S901 4-(Aminomethyl)phenol (OHBA)	S902 4-Methylbenzylamine (MeBA)	S903 cis-1,2-Cyclohexanediamine	S904 trans-1,3-Cyclohexanediamine	S905 1,5-Diaminopentane (C5dami)
				
S906 1,7-diaminoheptane	S907 4-Aminobenzylamine	S908 2-Ethylhexylamine	S909 2-(Methylthio)ethylamine	

These guest molecules were not used in the training and test datasets for the model construction.

Structural analysis for the new layered PDAs

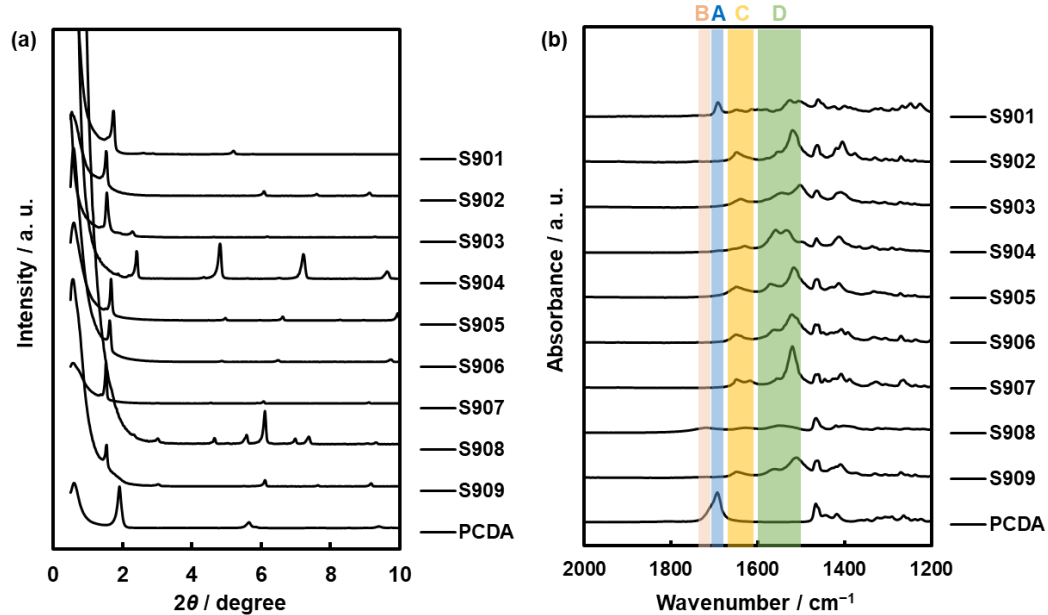


Fig. S6. XRD patterns (a) and FT-IR spectra (b) of the newly synthesized layered PDA with the intercalation of the guests **S901–S909**.

The original PCDA without the guest showed the interlayer distance (d_0) = 4.66 nm. The peak shift indicating the intercalation of the guests was observed for all these guests (Fig. S6a). The observed d_0 was as follows: (a) 5.08 nm for **S901**, 5.77 nm for **S902**, 6.28 nm for **S903**, 3.61 nm for **S904**, 5.29 nm for **S905**, 5.42 nm for **S906**, 5.80 nm for **S907**, 5.79 nm for **S908**, 5.75 nm for **S909**. In FT-IR spectra (Fig. S6), the changes in the carboxy and amine groups were observed for all these guests. Please see the explanations in Fig. S2.

T - Δx relationship for the new layered PDAs

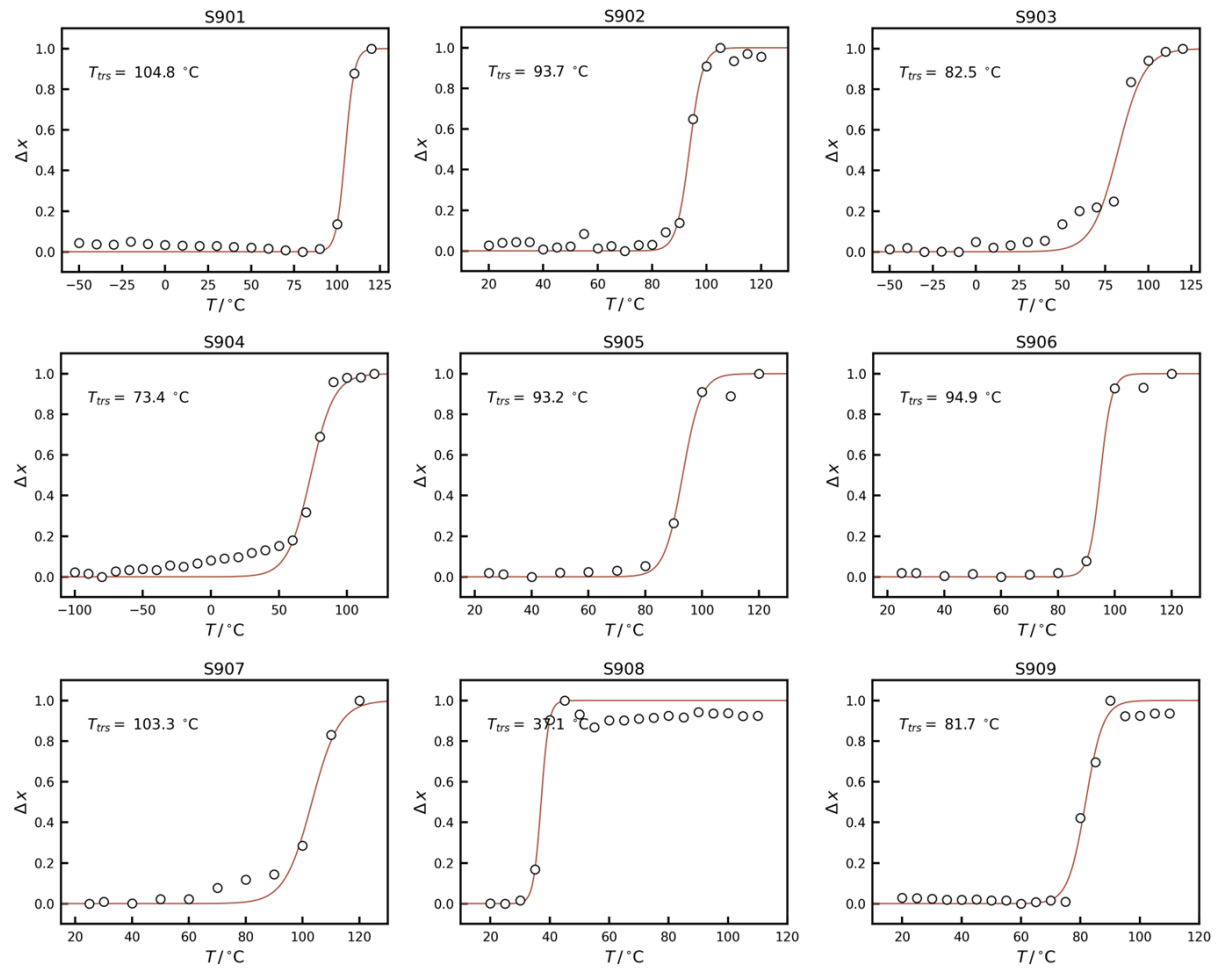


Fig. S7. T - Δx relationship (plot), its approximation using sigmoidal function (red line), and calculated T_{trs} for the newly synthesized layered PDA (S901–S909) for the experimental validation.